WWW.IJRPR.COM

International Journal of Research Publication and Reviews

Journal Homepage: www.ijrpr.com ISSN 2582-7421

Modelling and Closed-Loop Control of a Two-Stage Three-Phase Grid-Connected Solar PV Inverter

Malothu Vishnu Vardhan[1], Prof. G.V.Siva Krishna Rao[2]

[1]Mtech Student, Dept. of Electrical Engineering, Andhra University, Visakhapatnam, India. Email: mv.vardhan.malothu@gmail.com
[2]Professor, Dept. of Electrical Engineering, Andhra University, Visakhapatnam, India. Email: gvskrishna_rao@yahoo.com

ABSTRACT

The new age of electricity generation is renewable energy. There is no other room, but to use renewable resources in energy generation to make the planet safer, and sustainable for the future. Renewable resources come in a variety of ways, but solar energy is by far the most practical. These days, solar panels are widely used due to their ease of use, accessibility, and efficiency in producing power. The Paper begins with a comprehensive review of existing literature on grid-tied inverters, including their functionalities, control strategies, and integration challenges. Based on this review, a novel topology is proposed, which incorporates perturb and observe technique and power electronics techniques to maximize energy conversion efficiency and grid stability. This Paper mainly represents the simulation of compact design of a grid-tied solar system for energy production using Maximum power point tracking. Several fundamental characteristics, including temperature, irradiance, voltage, and current, affect the efficiency of a solar panel. Hence sudden change in any of these parameters leads drop in power and voltage. The precept aim is to improve the output voltage of PV array and boost converter there by reducing the harmonic content in grid current. In this paper, MATLAB/Simulink software is used to simulate and analyse the operation of a PV array integrated with the utility grid through a two-stage power conversion system. This paper contributes to the ongoing efforts to enhance the performance and reliability of grid-tied inverters for solar PV applications.

Keywords: Solar Photovoltaic (PV), Grid-Connected Inverter, Two-Stage Power Conversion, Maximum Power Point Tracking (MPPT), Perturb and Observe (P&O). Boost Converter, Three-Phase Inverter, Grid Integration, Harmonic Reduction.

1. INTRODUCTION:

Two-stage grid-connected photovoltaic systems are widely used for both scale and small-scale power generation. Their performance is highly dependent on variations in the amount of radiation and temperature. The dynamics of these systems under changing weather conditions can be analyzed using closed-loop control methods to ensure continuous delivery of energy to the power grid in the face of changes. In recent years, machine learning has been used effectively to model complex power electronic systems without necessarily using complicated physical equations. Of all the various machine learning techniques, supervised learning proves to be effective since it learns from experience. Forecast the dynamic response of a closed-loop grid-tied solar PV system. It continually improves the parameters of the model to make its predictions more accurate, making it suitable for

nonlinear systems. The PV array under investigation consists of one string with six 1Soltech 1STH-350-WH modules connected in series. All modules have open circuit voltage of 51.5 V and short circuit current of 9.4 A. The ideality factor of diode is 1.045 and saturation current of diode is 0.323 nA. The series resistance of parasitic nature is 0.22 Ω and shunt resistance is 47.96 Ω. The primary objective of this analysis is the comparison of predicts system behavior with closed loop simulation, particularly under abrupt changes in irradiance and temperature. Performance is evaluated by means of two parameters – output voltage of DC-DC boost converter and current fed to utility grid. These metrics help assess the stability of the feedback control system and the efficiency of the converter. The results provide a computational basis for improving power electronic designs that interface, with the grid.

2. PROPOSED SYSTEM:

The proposed grid-interfaced photovoltaic system is built using a dual-stage power conversion design. This setup separates the task of extracting power from the solar panels from the job of syncing with the grid. The energy flows step by step from the PV array to a DC-DC boost stage then through an intermediate DC-link bus. After that it moves to a three-phase voltage source inverter followed by a LCL filter. Finally the power connects to the utility grid at the Point of Common Coupling..

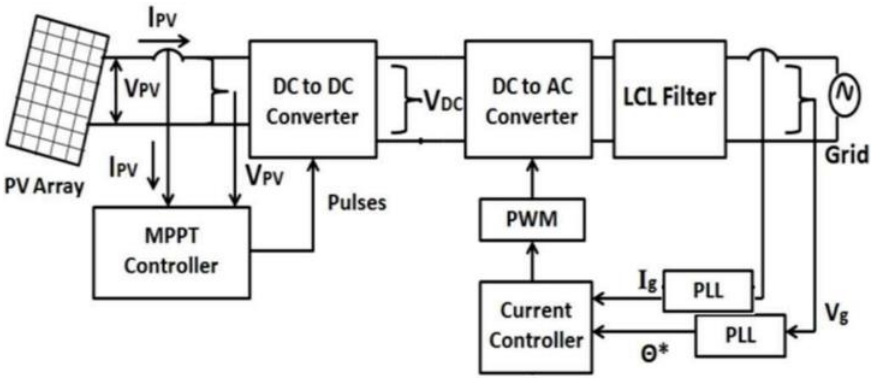


Figure 1: Proposed System

3. PHOTOVOLTAIC ARRAY MODELING:

3.1 PV Cell Model

A photovoltaic (PV) cell directly converts solar light that falls on it into electrical energy by means of the photovoltaic effect. To analyse the behaviour of a PV cell in dynamic simulation and in power-electronic interfaces engineers model the PV cell with a single-diode equivalent circuit. A shunt resistance is added to represent leakage paths and a series resistance represents the resistance of metal contacts and of the bulk semiconductor. By applying Kirchhoff's Current Law to the circuit one arrives at a nonlinear implicit current-voltage (I–V) equation that describes the PV cell.

$$I = IL - I0[\exp\{q(V + IRs)/(nkT)\} - 1] - (V + I_{rs})/r_{sh} \quad (1)$$

$$P_{PV} = V_{PV}\, I_{PV} \quad (2)$$

$$P_{MPP} = V_{MPP}\, I_{MPP} \quad (3)$$

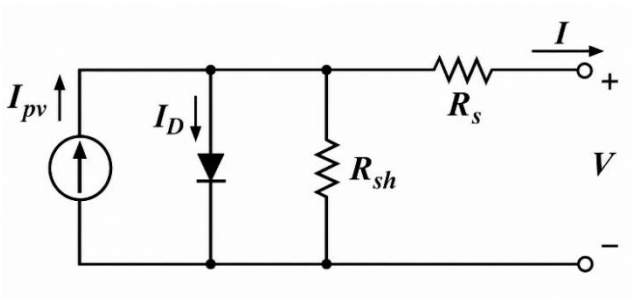


Figure 2: Equivalent Circuit of Solar Cell

4. MAXIMUM POWER POINT TRACKING

4.1 Perturb and Observe Method

To make sure we keep getting the power possible even when the weather changes we use a special method called Perturb and Observe. This method is also known as P&O. It helps control the way the solar panel works. The system checks the voltage and the current from the panel every time it switches. It then uses those numbers to find out how power the panel is making. The system changes the voltage a bit and sees if the power goes up or down. It keeps doing this over again. The goal is to find the point where the solar panel can make the most power. The system looks at the difference in power and the difference, in voltage to decide what to do.

$$\Delta V = V(k) - V(k-1) \quad (4)$$

$$\Delta P = P(k) - P(k-1) \quad (5)$$

$$V_{ref}(k) = V_{ref}(k-1) \pm \Delta V_{step} \quad (6)$$

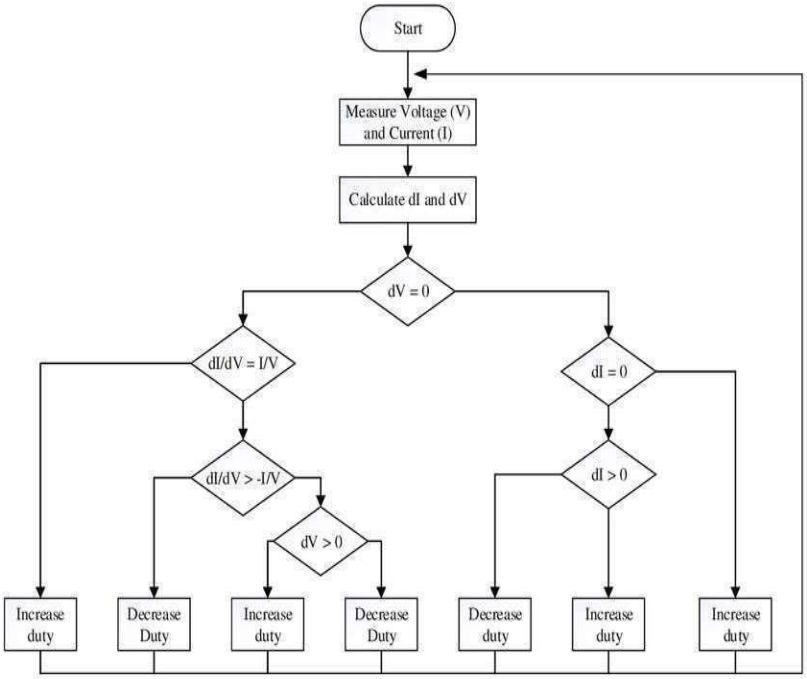


Figure 3: Flow Chart of P & O Algorithm

5. DC-DC BOOST CONVERTER:

A step-up DC-DC boost topology is the front-end interface that lifts the terminal voltage of the solar PV array to the nominal voltage level needed at the intermediate DC-link bus. The power stage architecture has an input filtering and energy-storage inductor, a pulse-width-modulated (PWM) semiconductor switch, a unidirectional rectifying diode and an output DC-link filter capacitor that connects to the load stage. If we assume a lossless circuit that works in Continuous Conduction Mode (CCM) the steady-state relationship, between the input PV voltage and the stepped-up DC-link output voltage is expressed as…

$$V_{dc} = V_{PV} / (1 - D) \quad (7)$$

$$D = 1 - V_{PV} / V_{dc} \quad (8)$$

$$V_L = V_{PV} \quad (9)$$

$$V_L = V_{PV} - V_{dc} \quad (10)$$

$$DV_{PV} + (1 - D)(V_{PV} - V_{dc}) = 0 \quad (11)$$

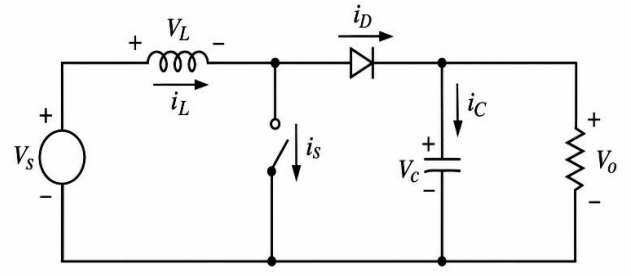


Figure 4: Boost Converter Circuit

6. THREE-PHASE GRID-SIDE INVERTER:

This stage uses a three-phase full-bridge Voltage Source Inverter (VSI) topology. The VSI takes the DC-link bus voltage and turns it into grid-compatible three-phase AC power. To make a sinusoid with few harmonics the inverter switches – there are six of them – are driven by gating pulses created with a Sinusoidal Pulse-Width Modulation (SPWM) technique. In this SPWM setup the closed-loop inverter controller produces three sinusoidal modulating signals. These signals run at the frequency and are offset by 120(2pi/3rad) from each other. The three-phase reference waveforms are fed at the time into fast comparators together with a shared high-frequency triangular carrier wave. Where the low-frequency sinusoidal references cross the high-frequency

carrier the comparators mark the moments when the switches must turn on or off. Those moments set the duty-cycle variations, for each inverter phase leg. The result is a set of gate-drive signals that mimic the desired fundamental AC waveform right at the inverter terminals.

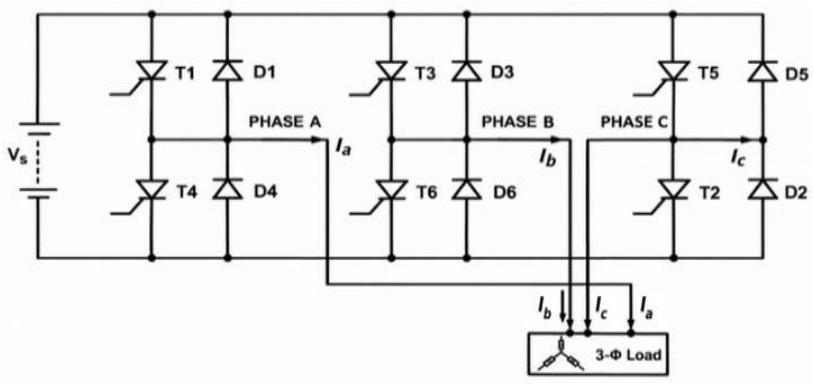


Figure 5: Circuit Diagram Of Three Phase Inverter

$$va^* = Vm \sin(\omega t) \quad (12)$$

$$vb^* = Vm \sin(\omega t - 120°) \quad (13)$$

$$vc^* = Vm \sin(\omega t + 120°) \quad (14)$$

7. GRID SYNCHRONIZATION AND CONTROL:

7.1 Phase-Locked Loop

Accurate synchronization between the three-phase Voltage Source Inverter and the utility network is controlled by a Synchronous Reference Frame Phase-Locked Loop. This system constantly follows the real-time phase angle of the grid voltage vector. The synchronization process performs a two-step coordinate transformation on the three-phase point-of-coupling voltages. First the changing three-phase grid voltages are moved to a two-axis stationary coordinate system through the Clarke transformation. Then these stationary voltage parts are moved into a rotating reference frame using the Park transformation. The feedback phase angle is used for this step. By making sure the quadrature-axis voltage component is zero the system locks in phase with the voltage. This gives an angular reference, for the current controller.

$$V\alpha = (2/3)(Va - Vb/2 - Vc/2) \quad (15a)$$

$$V\beta = (Vb - Vc)/\sqrt{3} \quad (15b)$$

$$V_d = V_\alpha \cos\theta + V_\beta \sin\theta \quad (16)$$

$$V_q = -V_\alpha \sin\theta + V_\beta \cos\theta \quad (17)$$

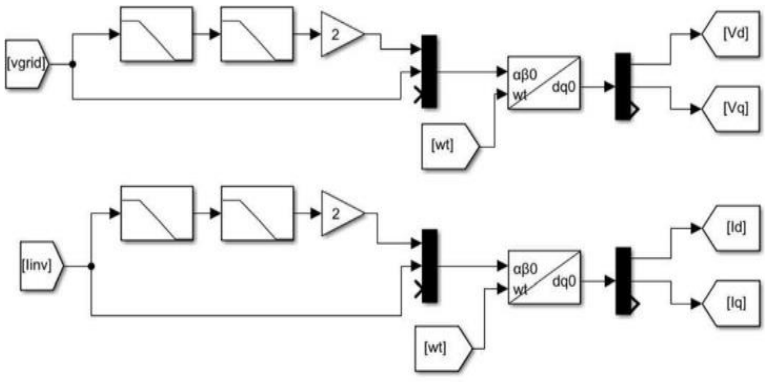


Figure 6: Phase-Locked Loop

7.2 Feed-Forward Decoupling Control

To achieve zero steady-state tracking error and a quick transient response I regulate the grid-side inverter in a synchronous d–q reference frame that is aligned with the utility voltage vector. Using the state-space voltage balance across the output filter stage I formulate the relationship that governs the inverter terminal voltages in the rotating frame.

$$V_{inv},d = V_g,d + R\ I_d + L(dI_d/dt) - \omega\ L\ I_q \quad (18)$$

$$V_{inv},q = V_g,q + R\ I_q + L(dI_q/dt) + \omega\ L\ I_d \quad (19)$$

Because the speed-dependent rotational voltages create cross-coupling between the active and reactive control axes I insert feedforward decoupling terms at the output of the Proportional-Integral (PI) regulators. This compensation eliminates cross-axis disturbances. Gives me independent first-order control over the d-axis and q-axis currents. When I inject power with unity power factor I keep the current command at zero ($I_q^* = 0$) which forces the injected AC current to stay strictly in phase, with the grid voltage.

$$I_q^* = 0 \quad (20)$$

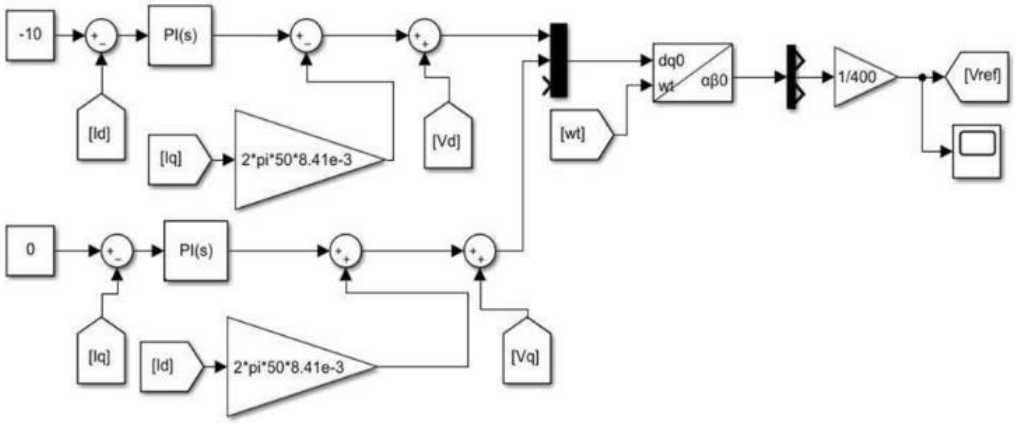


Figure 7: Feed-Forward Decoupling Control

8. LCL FILTER:

In the two-stage PV system that connects to the power grid a third-order LCL harmonic filter is placed between the three-phase Voltage Source Inverter and the grid. Each phase of the filter has a T-shape setup. It includes an inductor on the side a capacitor for filtering and an inductor on the grid side. This filter is located before the Point of Common Coupling. It helps separate the inverter from the grid and stops high-frequency harmonic currents from entering the grid. Even though the three-phase VSI makes AC power, from the DC bus, the high-frequency PWM switching creates a lot of distortion. The LCL setup reduces these harmonics by sending high-frequency current through the capacitor, which has resistance. It stops the current from going into the grid using the inductors. As a result the filter gives an smooth current at the grid. This makes the power quality better. Lowers the total harmonic distortion.

The resonance frequency of the LCL filter is expressed as:

$$f_{res} = (1/2\pi)\sqrt{[(L_1 + L_2)/(L_1L_2C_f)]} \quad (21)$$

where L_1 is the inverter-side inductance, L_2 is the grid-side inductance, and C_f is the filter capacitance. The LCL filter is therefore an important part of the proposed system because it enables the controlled power generated by the PV array to be injected into the three-phase grid with reduced switching harmonics.

9. SYSTEM PARAMETERS

The parameters of the PV array, the boost converter and the grid-side inverter used in the simulation are given in Tables I, II, and III.

TABLE I

PV ARRAY PARAMETERS

Parameter	**Value**
PV module	1Soltech 1STH-350-WH
Number of series modules	6
Number of parallel strings	1
Open-circuit voltage	51.5 V
Short-circuit current	9.4 A

Parameter	**Value**
Series resistance	0.22 Ω
Shunt resistance	47.96 Ω
Diode ideality factor	1.045
Diode saturation current	0.323 nA

TABLE II

GRID-SIDE INVERTER PARAMETERS

Parameter	**Value**
System rating	100 kVA
DC-link voltage	585–600 V
Grid voltage	400 V RMS
Grid current	141.49 A RMS
Grid configuration	Three-phase
Filter	LCL
Synchronization	PLL (synchronous reference frame)
Current control	Feed-forward decoupling (d–q frame)

TABLE III

BOOST CONVERTER PARAMETERS

Parameter	**Value**
Input voltage (PV array)	303.6 V at the MPP (reference limit 363 V)
Output / DC-link voltage	Approximately 600 V
Switching frequency	10 kHz
Operating mode	Continuous conduction
MPPT method	Perturb and Observe (P&O)

10. SIMULATION RESULTS AND DISCUSSION:

10.1 PV Characteristics

The time-domain simulation of the photovoltaic array shows that the I-V and P-V electrical characteristics are very nonlinear across the range of operating voltages. As shown in the simulated array profiles under the given conditions the PV generator reaches a steady-state operating point of about 303.6 V and 356.26 A. This results in a power generation capacity of about 100 kW at the Maximum Power Point.

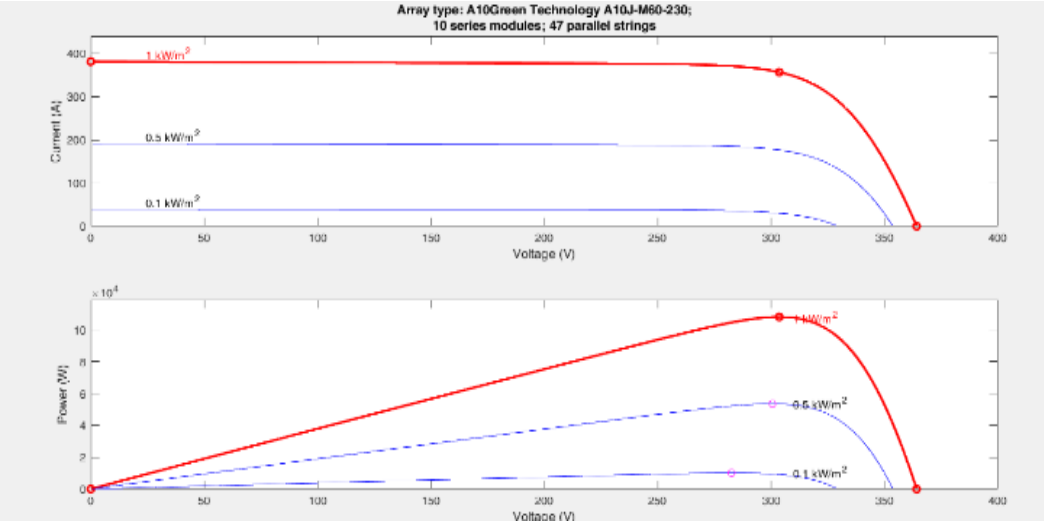


Figure 8: Current Voltage and Power Voltage Curves

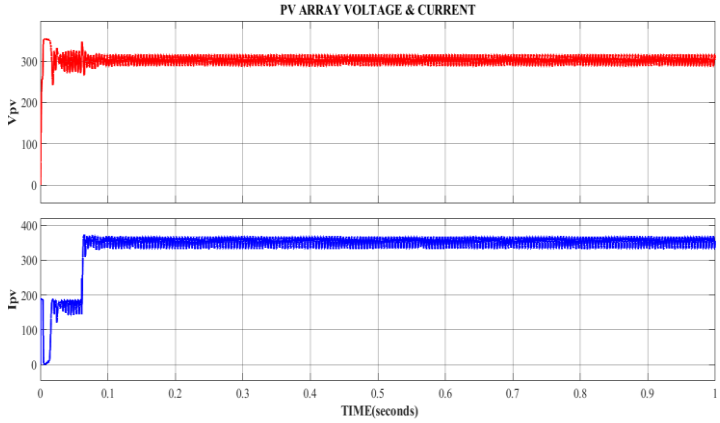


Figure 9: PV Array Curves

10.2 Inductor Current Waveform

The current that moves through the energy-storage inductor in the step-up DC-DC converter is shown below. Since the inductor current never goes to zero during the time the switch is turning on and off the shape of the wave shows that energy is always being moved and proves that the system is working in Continuous Conduction Mode. Also the highest frequency current variation is kept to 10% of the normal inductor current, which reduces the loss in the magnetic part and the copper part of the inductor. This also stops much current variation from affecting the solar PV array terminals.

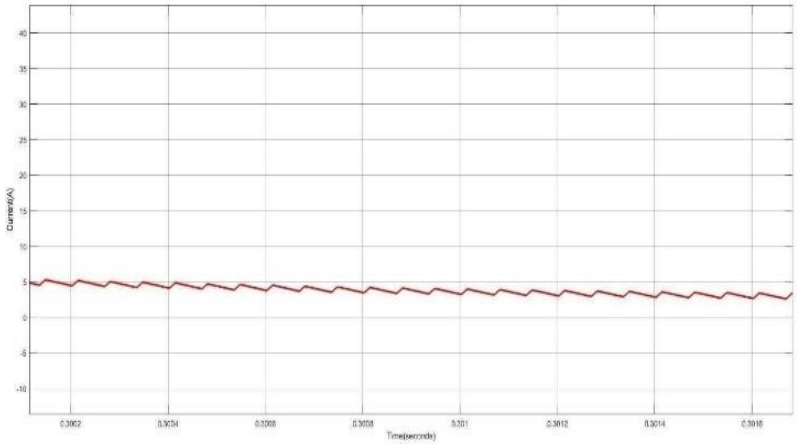


Figure 10: Boost Converter Inductor Current

10.3 Case 1: Standard Test Conditions

To establish baseline steady-state performance the closed-loop PV conversion system is first simulated under Standard Test Conditions. The environmental inputs are set to a fixed irradiance of 1000 W/m² and an operating temperature of 25°C. The simulation shows how the front-end boost topology increases the PV array voltage to an output of 600 V DC across the DC-link. The voltage stays steady over time with little fluctuation. The ripple, in the steady-state voltage is 3 V, which equals a 0.5% ripple factor. This small level of ripple confirms that high-frequency voltage oscillations are minimal before the system converts DC power to AC.

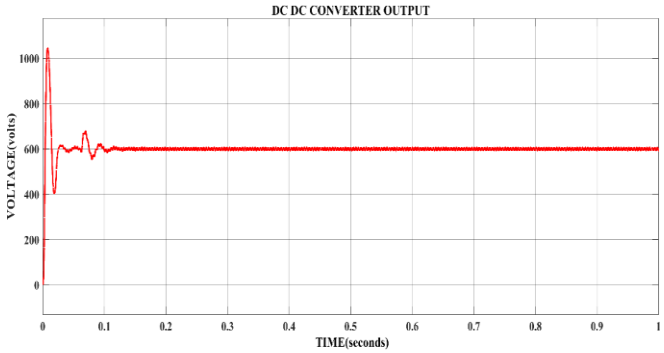


Figure 11: Boost Converter Output Voltage Case-1

10.4 Case 2: Change in Sunlight Intensity

In this test scenario the PV array temperature is kept at 25 °C to create an isothermal operating condition. The solar irradiance is varied over time to mimic cloud transients. The simulated converter response shows that the boost stage maintains the intermediate DC-link bus at 400 V DC with a voltage ripple of only 3 V, which is a 0.75 % ripple factor. When the solar irradiance experiences a step change the boost converter output drops momentarily revealing a brief settling interval. This brief settling interval is required by the P&O MPPT and the feedback control loops to rebalance power flow, across the DC link.

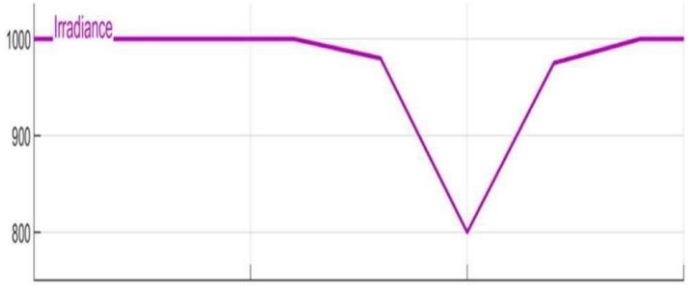


Figure 12: Change in Sunlight Intensity

10.5 Case 3: Change in Heat

In the operating scenario the environmental test conditions are reversed. Solar irradiance is held constant at 1000 W/m² throughout the simulation. At the time ambient temperature is varied in dynamic steps over the simulation period. Under these changing conditions the front-end boost converter maintains a stable output of 400 V DC across the DC-link capacitor. The voltage stays within a 3 V ripple margin, which corresponds to a 0.75% factor during steady-state operation.

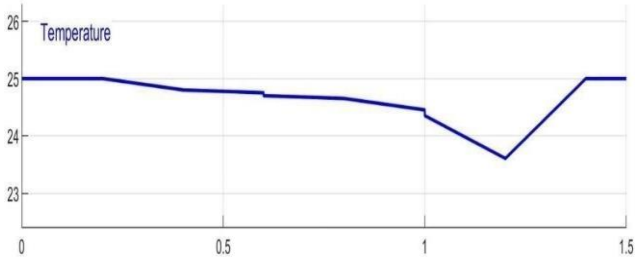


Figure 13: Change in Heat

10.6 Grid Current

I observe that the superimposed time-domain waveforms of the utility grid voltage and the injected inverter current show that the two quantities remain tightly in phase throughout the entire AC cycle. This zero-phase-shift relationship tells me that the closed-loop inverter controller successfully keeps the reactive-current command at zero (Iq= 0) inside the rotating d–q reference frame. Because of this reactive power no longer moves between the Voltage Source Inverter (VSI) and the utility grid. This shows that the two-stage conversion system injects real power into the utility grid and it operates at unity power factor.

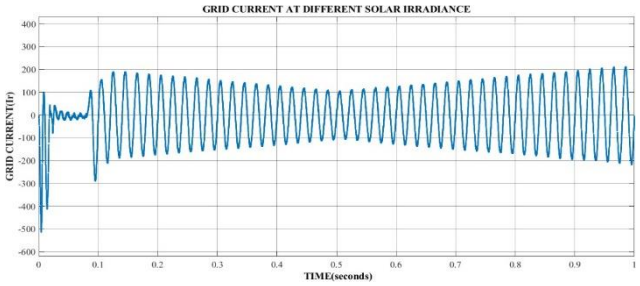


Figure 14: Grid Current Waveform

10.7 Grid Voltage and Current

I observe that the superimposed time-domain waveforms of the utility grid voltage and the injected inverter current show that the two quantities remain tightly in phase throughout the entire AC cycle. This zero-phase-shift relationship tells me that the closed-loop inverter controller successfully keeps the reactive-current command at zero (Iq= 0) inside the rotating d–q reference frame. Because of this reactive power no longer moves between the Voltage Source Inverter (VSI) and the utility grid. This shows that the two-stage conversion system injects real power into the utility grid and it operates at unity power factor.

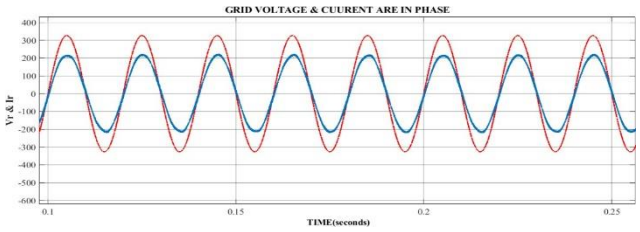


Figure 15: Grid Voltage and Current in Phase

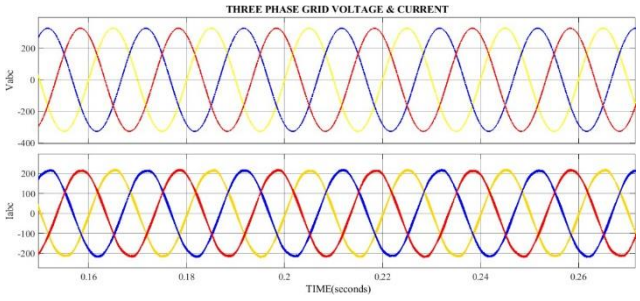


Figure 16: Three phase grid voltage and current

10.8 Solar Irradiance vs Power

The simulation result for the power curve shows that the power generation by the PV panel happens in a manner that corresponds to variations in the solar irradiation. The reaction is almost instantaneous, implying that the system can react instantly to changes in the solar energy. This instantaneous reaction shows that the DC-DC converter controlled using the MPPT algorithm operates satisfactorily in a closed loop environment.

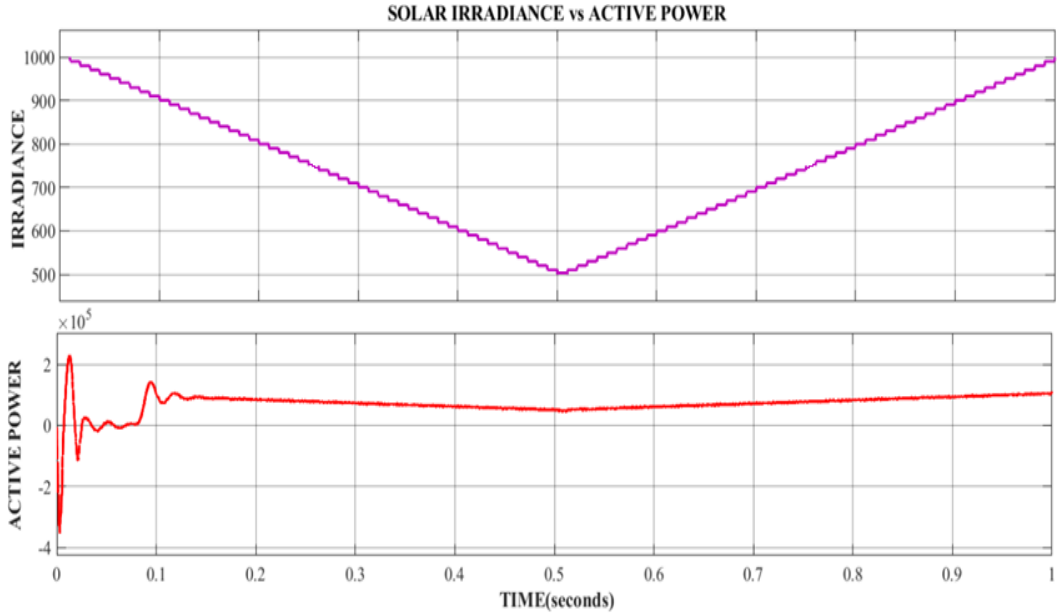


Figure 17: Solar Irradiance v/s Power

10.9 THD Analysis

The harmonics spectrum and purity of the injected AC current is analyzed using Fast Fourier Transform (FFT) based frequency domain technique. The THD of the injected AC current obtained from the simulated harmonics spectrum of the closed loop system is:

THD = 4.123%

A distortion factor less than the 5% limit defined by the grid code standard shows that the current being injected into the system meets the power quality specifications for the utility company. This is realized through the implementation of the closed-loop feedforward current control scheme and third order LCL filter circuitry, which attenuates both the switching ripples and harmonics.

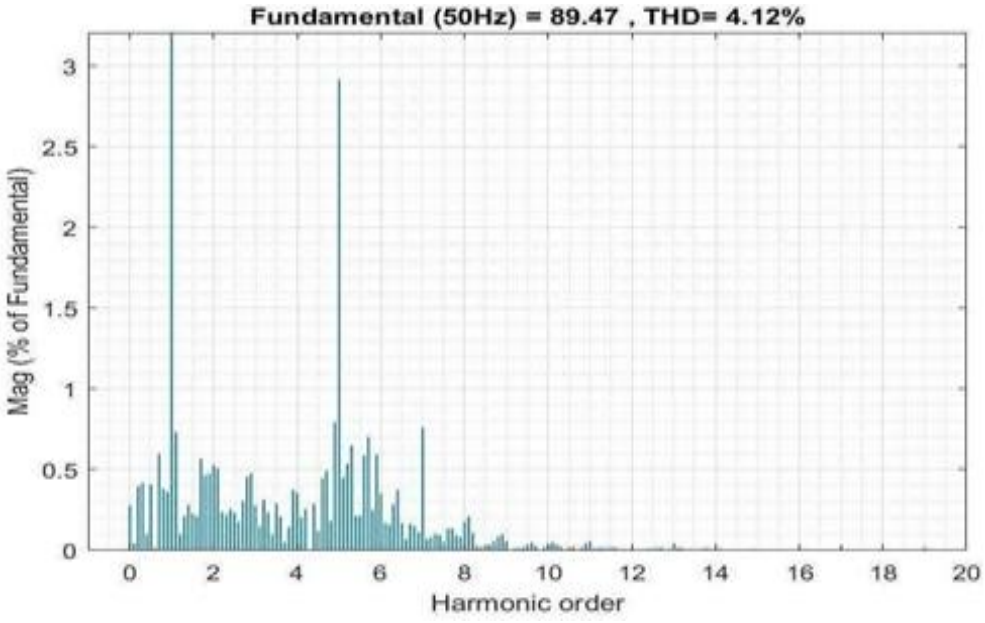


Figure 18: THD Analysis of Grid Current

11. OVERALL PERFORMANCE AND COMPARISON WITH THE REFERENCE PAPER

Table IV summarises the main simulation results of the proposed system.

TABLE IV

SIMULATION PERFORMANCE RESULTS

Parameter	**Value**
PV voltage	303.6 V
PV current	356.26 A
PV power	Approximately 100 kW
DC-link voltage	585–600 V
Grid voltage	400 V RMS
Grid current	141.49 A RMS
Grid-current THD	4.123 %
Settling time	0.025 s

The proposed system operates around the maximum power point while keeping the DC-link voltage close to its target. The grid current is nearly sinusoidal, and the voltage–current phase relationship shows controlled injection of active power. Table VI compares the proposed system with the reference grid-connected PV system.

TABLE V

COMPARISON OF THE PROPOSED SYSTEM WITH REFERENCE

PAPER

Parameter	**Reference paper**	**Proposed system**
Simulation software	PSIM	MATLAB/Simulink
System rating	360 W (six 60 W panels)	About 100 kW
PV array voltage	100 V	303.6 V
DC-DC converter	Boost, 100 V to 150 V	Boost, 303.6 V to about 600 V
Converter switching frequency	30 kHz	10 kHz
MPPT method	Perturb and Observe	Perturb and Observe
Inverter	Single-phase full H-bridge, SPWM	Three-phase full-bridge VSI, SPWM
Output filter	L filter (5 mH)	LCL filter
Grid	110 V, 60 Hz, single-phase	400 V RMS, three-phase
Grid synchronization	Conventional single-phase PLL	Synchronous-reference-frame PLL (Clarke/Park)
Current control	PI controller; reference from MPPT power	d–q PI control with feed-forward decoupling, Iq =0
Test conditions	Irradiance 800 and 1000 W/m² at 25 °C	STC, irradiance change and temperature change
Power-quality result	Sinusoidal grid current; THD not reported	THD = 4.123 % (below 5 %)

Compared with Reference paper, the proposed system is a three-phase system of much higher power, it uses an LCL filter instead of an L filter, it controls the active and reactive currents independently in the d–q frame, and it reports a quantitative power-quality figure (THD) in addition to the sinusoidal current waveform. Both systems use P&O MPPT with a boost converter, so the MPPT stage is directly comparable.

12. CONCLUSION

Based on the simulation results of the Grid tied Solar System using maximum power point technique, it can be concluded that Closed loop operation method is capable of predicting the output voltage of Boost Converter and grid current under different input conditions of sudden changes in irradiance and temperature. When there is change in the solar irradiation the maximum power point changes and thus the required duty cycle for the operation of the model also changes. So MPPT Algorithm is used to track Maximum Power Point Continuously. The PV module introduces harmonic content in current and voltage and the output of the PV was also affected considerably. A Synchronous Frame PLL (SFPLL) is used for synchronization for single phase signals with acceptable results. In the specific case of sudden changes in both temperature and irradiance, to closed loop operation, drop in output voltage of boost converter is minimized by perturb and observe technique. Grid Current THD is also less than 5%.

REFERENCES

1. Motan Noureddin, Muhammad Abu-Khaizaran, and Mahran Quraan. "Photovoltaic array modelling and boost-converter controller-design for a 6kW grid-connected photovoltaic system-DC stage." In 2018 IEEE International Conference on Environment and Electrical Engineering and 2018 IEEE Industrial and Commercial Power Systems Europe (EEEIC/I&CPS Europe), pp. 1-6. IEEE, 2018.
2. Pham Dung H., Gregory Hunter, Li Li, and Jianguo Zhu. "Feedforward decoupling control method in grid-interfaced inverter." In 2013 Australasian Universities Power Engineering Conference (AUPEC), pp. 1-5. IEEE, 2013.
3. Bowtell L, and Tony Ahfock. "Comparison between unipolar and bipolar single phase grid connected inverters for PV applications." In 2007 Australasian Universities Power Engineering Conference, pp. 1-5. IEEE, 2007.
4. Bhagali Priyal, and R. K. Thakur. "Design of DC–DC Boost Converter for Solar Photovoltaic Systems Based on Monthly Averaging of Irradiance & Temperature." In 2022 IEEE Sustainable Power and Energy Conference (iSPEC), pp. 1-5. IEEE, 2022.
5. Shadoul, Myada, Rashid Al Abri, Hassan Yousef, and Mahmoud Masoud. "DC-DC boost converter controller design for PV applications." In 2017 9th IEEE-GCC Conference and Exhibition (GCCCE), pp. 1-6. IEEE, 2017.
6. Elbaset Adel A, M. S. Hassan, and Hamdi Ali. "Performance analysis of grid- connected PV system." In 2016 Eighteenth International Middle East Power Systems Conference (MEPCON), pp. 675-682. IEEE, 2016.
7. M. Hajihosseini, M. Andalibi, M. Gheisarnejad, H. Farsizadeh and M. Khooban, DC/DC Power Converter Control-Based Deep Machine Learning Techniques: Real- Time Implementation, in IEEE Transactions on Power Electronics, vol. 35, no. 10, pp. 9971- 9977, Oct. 2020, doi:10.1109/TPEL.2020.2977765.
8. Gudey Satish Kumar, and Rajesh Gupta. "Recursive fast terminal sliding mode control in voltage source inverter for a low-voltage microgrid system." IET Generation, Transmission & Distribution 10, no. 7 (2016): 1536-1543.
9. Güler Naki, and Erdal Irmak. "MPPT based model predictive control of grid connected inverter for PV systems." In 2019 8th International Conference on Renewable Energy Research and Applications (ICRERA), pp. 982-986. IEEE, 2019.
10. Bana Prabhat Ranjan, Simone Vanti, and Mohammad Amin. "Single-stage grid- connected pv system with artificial neural network controller." In 2021 IEEE 22nd Workshop on Control and Modelling of Power Electronics (COMPEL), pp. 1-7. IEEE, 2021.